Available online at www.sciencedirect.com
ScienceDirect
Trans. Nonferrous Met. Soc. China 20(2010) 1387−1391
Transactions of Nonferrous Metals Society of China
www.tnmsc.cn

# Mechanical properties of underwater friction stir welded 2219 aluminum alloy

LIU Hui-jie(刘会杰), ZHANG Hui-jie(张会杰), HUANG Yong-xian(黄永宪), YU Lei(于 雷)

State Key Laboratory of Advanced Welding Production Technology,
Harbin Institute of Technology, Harbin150001, China

Received 15 September 2009; accepted 24 December 2009

**Abstract**: Underwater friction stir welding of 2219 aluminum alloy was carried out in order to further improve the joint performances by varying welding temperature history. The results indicated that the tensile strength of the joint can be improved from 324 MPa by external water cooling action in normal to 341 MPa. However, the plasticity of the joint is deteriorated. The underwater joint tends to fracture at the interface between the weld nugget zone and the thermal mechanically affected zone on the advancing side during tensile test, which is significantly different from the normal joint.
**Key words***:* aluminum alloy; underwater friction stir welding; mechanical property

## 1 Introduction

Friction stir welding (FSW), as a solid state joining process, has been widely utilized to weld various aluminum alloys that were difficult to fusion weld[1−3]. Although the low heat input generated during FSW does not lead to the melting of the base metal, thermal cycles applied on the samples result in the reduction of mechanical properties of the joints[4−5]. Apparently, it is interesting and possible to improve the strength of normal friction stir welded joints by controlling the temperature level. External liquid cooling has been employed in several solid state joining processes to improve the joint performances. SARUKADA et al[6] studied the underwater friction welding of 6061 aluminum alloy by pressing a high-speed rotating cylindrical sample against another, and the results revealed that the joint had higher fatigue strength than that made in air. FRATINI et al[7] considered in-process heat treatment with water flowing on the plates during FSW, and significant improvement of ultimate tensile strength was observed in all the low, medium and high level of heat input controlled by variation of welding parameters. It was claimed that the reduction of soften zones caused by water cooling was responsible for the improvement in mechanical properties. Preceding investigations confirmed the feasibility of underwater friction stir welding to improve the mechanical properties of the joints. In this work, 2219 aluminum alloy was underwater friction stir welded and the tensile properties and fracture features of the joints were studied.

## 2 Experimental

The base material was a 2219 aluminum alloy plate of 7.5 mm thick, and the chemical composition and mechanical properties are listed in Tables 1 and 2. The plate was cut and machined into rectangular welding samples with a size of 300 mm×100 mm. Friction stir welding experiments were carried out in air and under water, respectively. For the convenience of statement, friction stir welding performed in air is defined as normal FSW, while the one performed under water is defined as underwater FSW. Fig.1 shows the schematic view of the underwater FSW. The samples were clamped to the backing plate in a vessel after being cleaned by acetone, and then water at room temperature was poured into the vessel to immerge the top surface of the samples. FSW was performed along the longitudinal direction of the samples using an FSW machine (FSW-3LM-003). The

**Foundation item:** Project(2010CB731704) supported by the National Basic Research Program of China; Project(2006BAF04B09) supported by the National Key Technology Research and Development Program of China; Project supported by the Program of Excellent Team in Harbin Institute of Technology, China
**Corresponding author:** LIU Hui-jie, Tel: 86-451-86413951; E-mail: liuhj@hit.edu.cn
DOI: 10.1016/S1003-6326(09)60309-5

welding tool and the parameters used in normal and underwater FSW were the same. The conical welding tool size and welding parameters are listed in Tables 3 and 4, respectively.

**Table 1** Chemical composition of 2219 aluminum alloy (mass fraction, %)

| Cu | Mn | Fe | Ti | V | Zn | Si | Zr | Al |
|---|---|---|---|---|---|---|---|---|
| 6.48 | 0.32 | 0.23 | 0.06 | 0.08 | 0.04 | 0.49 | 0.20 | Bal. |

**Table 2** Mechanical properties of 2219 aluminum alloy

| Ultimate strength/ MPa | 0.2% proof strength/ MPa | Elongation/ % |
|---|---|---|
| 432 | 315 | 11 |

**Table 3** Tool size used in FSW

| Shoulder diameter/mm | Pin diameter/ mm | Pin length/ mm | Tool tilt/ (°) |
|---|---|---|---|
| 22.5 | 7.5 | 7.4 | 2.5 |

**Table 4** Welding parameters used in FSW

| Rotation speed/ ($r \cdot min^{-1}$) | Welding speed/ ($mm \cdot min^{-1}$) | Axial pressure/ kN |
|---|---|---|
| 800 | 100 | 4.6 |

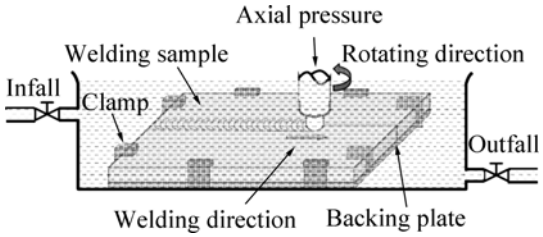


**Fig.1** Schematic diagram of underwater FSW

After welding, the joints were cross-sectioned perpendicular to the welding direction by an electrical-discharge cutting machine (DK-7718B-CG) for metallographic analyses and tensile tests. The cross-sections of the metallographic specimens were polished with a diamond paste, etched with Keller's reagent and observed by an optical microscopy (OM, Olympus-MPG3). The hardness (HV) was measured at the weld midplane of the metallographic specimens. The foil disk specimens for transmission electron microscopy (TEM, PHILIPS CM12) were cut from the base metal (BM) and the minimum-hardness location, and the electron transparent thin sections were prepared by double jet electro-polishing using a solution of 30% (volume fraction) nitric acid in methanol at 18 V and −35 ºC.

The configuration and size of the transverse tensile specimens were prepared with reference to Chinese National Standard (GB2625—89). The dimension of the tensile specimen is shown in Fig.2. The gage length used in tensile test is 50 mm. The room temperature tensile test was carried out at a crosshead speed of 1 mm/min using a computer-controlled testing machine (Instron-1186), and the results of each joint were evaluated using three tensile specimens cut from the same joint. After tensile test, the optical microscopy mentioned above and a scanning electron microscopy (SEM, Hitachi-S4700) were utilized to analyze the fracture features of the joints.

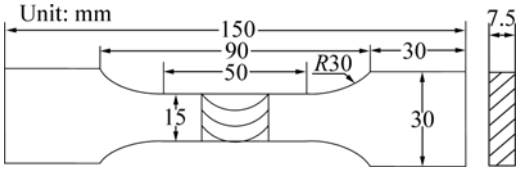


**Fig.2** Dimension of tensile specimen

## 3 Results and discussion

### 3.1 Tensile properties

The tensile properties of the joints are shown in Fig.3 and the error bars are based on the standard deviation. The normal joint has a tensile strength of 324 MPa, equivalent to 75% that of the base metal. Through underwater FSW, joints with tensile strength of 341 MPa can be produced, approximately 79% that of the base metal which is comparable to the maximum tensile strength obtained in normal condition[8]. Such a result indicates that the tensile strength of the joint can be improved by underwater FSW. However, the elongation of the underwater FSW joint only reaches 7.6% which is lower than that of the normal joint. The exact fracture locations of the joints are shown in Fig.4 in which the retreating side and the advancing side are denoted as RS and AS, respectively. Normal and underwater RSW joints exhibit quite different fracture features. The tensile specimens of the normal joint fracture in the heat affected zone (HAZ) near the interface between the

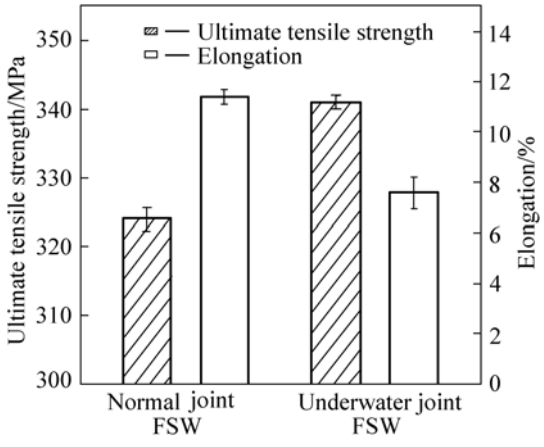


**Fig.3** Tensile properties of different joints

thermal mechanically affected zone (TMAZ) and HAZ on the AS (see Fig.4(a)), implying that the HAZ is the intrinsic weakest location of the joints; while the tensile specimens of the underwater joint fracture at the interface between the weld nugget zone (WNZ) and TMAZ on the AS (see Fig.4(b)), suggesting a strength improvement in the HAZ. Fig.5 presents the fracture surfaces of normal and underwater FSW joints, which further confirms the plasticity difference between the two joints. The fracture surface of the normal FSW joint is characterized by large dimples (Fig.5(a)), indicating that an extensive plastic deformation occurs during tensile test. However, dimple feature becomes ambiguous in the fracture surface of the underwater joint (Fig.5(b)), suggesting a decrease of plastic deformation level.

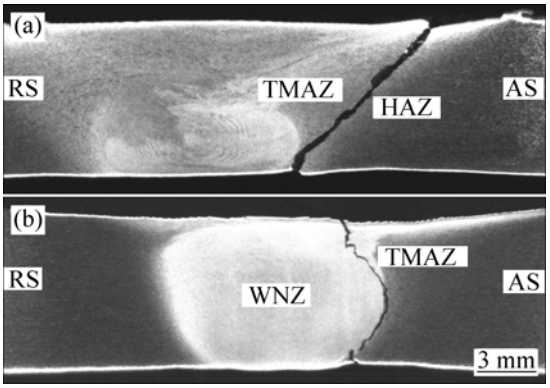


**Fig.4** Fracture locations of different joints: (a) Normal FSW; (b) Underwater FSW

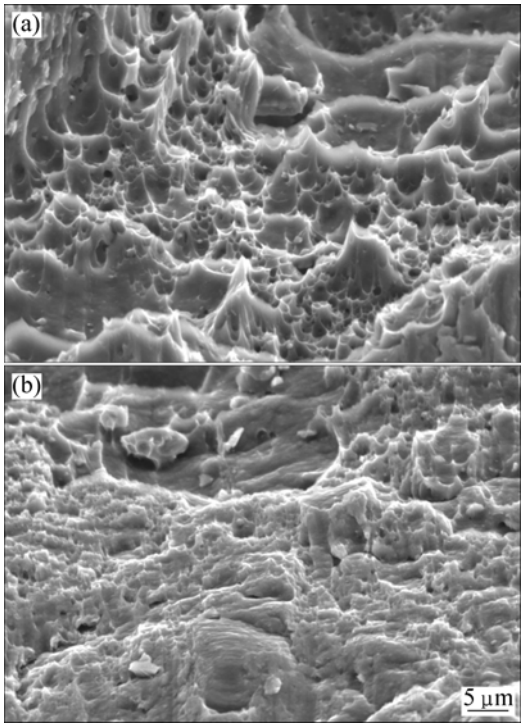


**Fig.5** Fracture surfaces of different joints: (a) Normal FSW; (b) Underwater FSW

### 3.2 Microhardness distributions

The micro-hardness distributions of the joints are shown in Fig.6. It is clear that a soften region consisting of the WNZ, TMAZ and HAZ is created in both normal and underwater FSW joints, which is a typical characteristic for FSW of precipitate hardened aluminum alloys[9−10]. For the normal joint, the hardness profile shows a "W-type" and the minimum hardness (HV 78−81) is in the HAZ on the AS, corresponding to the fracture location of the joint (Fig.4(a)). However, the hardness profile of the underwater joint exhibits quite different features. The soften region is remarkably narrowed, and the minimum hardness (HV 87−88) lies on the interface between WNZ and TMAZ on either side of the weld, which also coincides with the fracture location of the joint (Fig.4(b)). The minimum hardness of the underwater joint is higher than that of the normal joint, thus the tensile strength of the underwater joint is improved. In further observation, it is found that the underwater joint has lower hardness in the WNZ and higher hardness in the TMAZ and HAZ, which is contrast to the normal joint. As for precipitate-hardened aluminum alloy, it has been widely reported that the hardness of the joint is synthetically controlled by precipitate distribution, dislocation density, grain size and solid solution[11−13] which are all affected by external water cooling in the present study. Further microstructural analysis was carried out to reveal the tensile features of the joints.

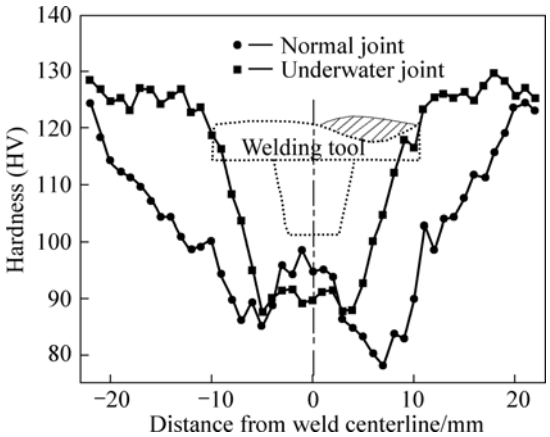


**Fig.6** Microhardness distributions of different joints

### 3.3 Microstructural analysis

The tensile properties depend closely on the microstructural characteristics of the weakest location of the joint. The microstructures in the minimum-hardness location (MHL) of the joints are shown in Figs.7 and 8. The MHL of normal joint has similar structure to that of the base metal (Figs.7(a) and (b)), while refined structures exist in the MHL of underwater joint (Fig.7(c)). On the other hand, the precipitates in the MHL of normal

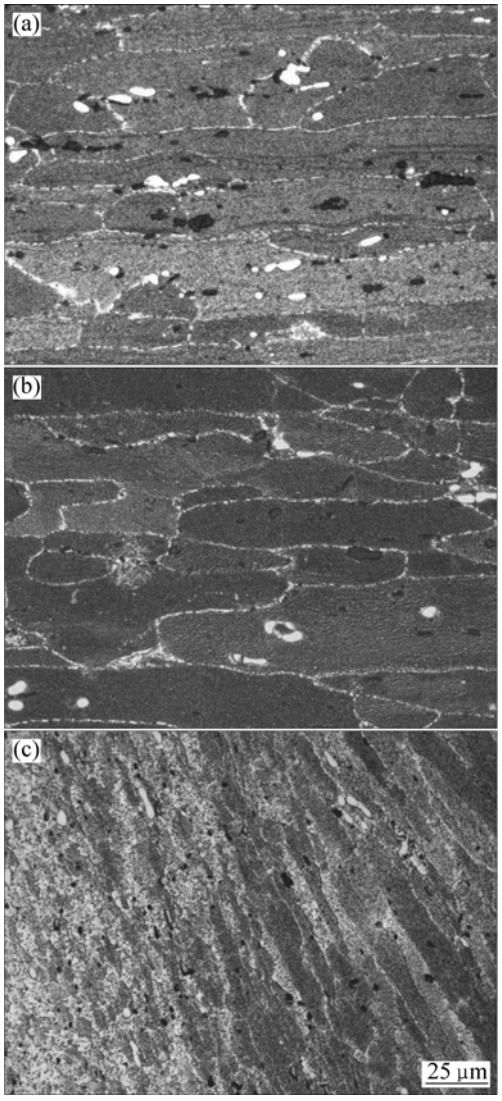


**Fig.7** SEM images of joints: (a) BM; (b) MHL of normal joint; (c) MHL of underwater joint

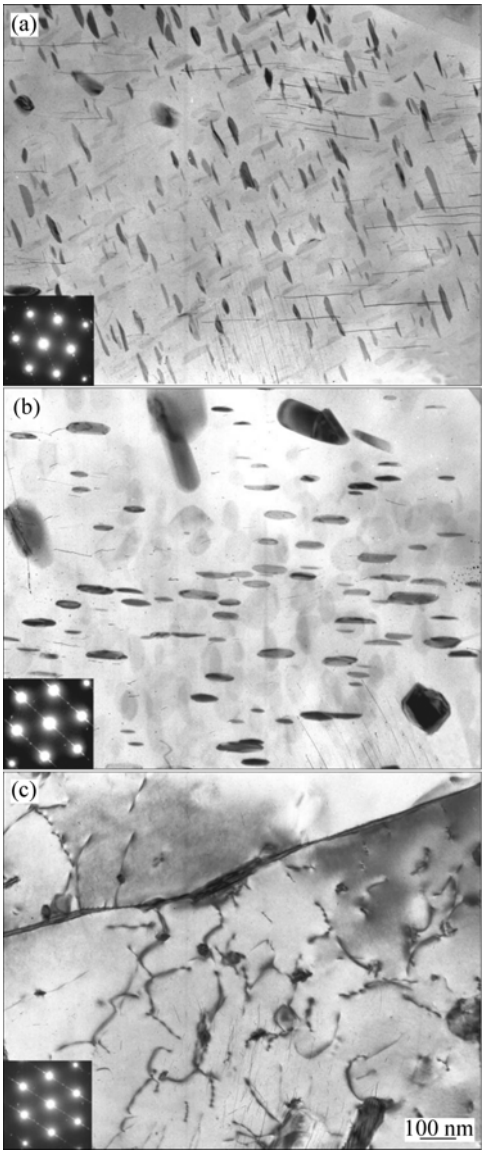


**Fig.8** TEM micrographs and selected area diffraction (SAD) patterns along $[110]_{Al}$ of aluminum matrix of precipitates in joints: (a) BM; (b) MHL of normal joint; (c) MHL of underwater joint

joint are significantly coarsened during FSW (Fig.8(a) and (b)), which greatly contributes to the decrease of hardness. In the MHL of underwater joint, although the precipitates are dissolved into the matrix in the welding thermal cycles, high-density dislocations are formed (see Fig.8(c)) as occurred in Refs.[14−15]. The dissolution of precipitates is beneficial to the solid solution strengthening. Therefore, the refined grain structures, high-density dislocations and enhanced solid solution strengthening effect synthetically lead to the increase of hardness of MHL, and thus improve the tensile strength of underwater joint.

For FSW joint, it is well known that the plastic deformation, especially the final necking, is mainly concentrated in the weakest region during tensile test [16−17]. Therefore, the elongation is dominantly determined by the latent plastic deformation ability of the weakest region of the joint. Regarding the underwater joint, the inhomogeneous deformation resistance caused by different grain orientations between the WNZ and TMAZ, the weakening of plastic deformation ability induced by high-density dislocations, together with the narrowing of the soften region should account for the decrease of elongation.

## 4 Conclusions

1) The tensile strength of the joint is improved, whereas the plasticity is deteriorated by underwater FSW.

2) The underwater FSW joint tends to fracture at the

interface between WNZ and TMAZ on the AS during tensile test, while the normal joints fracture in the HAZ on the AS.

3) Compared with the normal FSW joint, the underwater FSW joint exhibits lower hardness in the WNZ and higher hardness in the TMAZ and HAZ.

## References


[1] JOHNSEN M R. Friction stir welding takes off at Boeing [J]. Welding Journal, 1999, 78(2): 35−39.

[2] JOELJ D. The friction stir welding advantage [J]. Welding Journal, 2001, 80(5): 30−34.

[3] MISHRA R S, MA Zong-yi. Friction stir welding and processing [J]. Material Science and Engineering R, 2005, 50(1/2): 1−78.

[4] SVENSSON L E, KARLSSON L, LARSSON H, KARLSSON B, FAZZINI M, KARLSSON J. Microstructure and mechanical properties of friction stir welded aluminium alloys with special reference to AA 5083 and AA 6082 [J]. Science and Technology of Welding and Joining, 2000, 5(5): 285−296.

[5] STARINK M J, SESCHAMPS A, WANG S C. The strength of friction stir welded and friction stir processed aluminium alloys [J]. Scripta Materialia, 2008, 58(5): 377−382.

[6] SARUKADA D, KATOH K, TOKISUE H. Underwater friction welding of 6061 aluminum alloy [J]. Journal of Japan Institute of Light Metals, 2002, 52(1): 2−6.

[7] FRATINI L, BUFFA G, SHIVPURI R. In-process heat treatments to improve FS-welded butt joints [J]. International Journal of Machine Tools and Manufacture, 2008, 10(3): 42−53.

[8] PAN Qing. Welding defects and mechanical properties of friction stir welded 2219 aluminum alloy joints [D]. Harbin: School of Material Science and Engineering, Harbin Institute of Technology, 2007. (in Chinese)

[9] ZHAO Yan-hua, LIN San-bao, HE Zi-qiu, WU Lin. Microhardness prediction in friction stir welding of 2014 aluminium alloy [J]. Science and Technology of Welding and Joining, 2006, 11(2): 178−182.

[10] SIMAR A, BŔECHET Y, MEESTER DE B, DENQUIN A, PARDOEN T. Microstructure, local and global mechanical properties of friction stir welds in aluminium alloy 6005A-T6 [J]. Material Science and Engineering A, 2008, 486(1/2): 85−95.

[11] GENEVOIS C, DESCHAMPS A, DENQUIN A. Quantitative investigation of precipitation and mechanical behaviour for AA2024 friction stir welds [J]. Acta Materialia, 2005, 53(8): 2447−2458.

[12] ATTALLAH M M, DAVIS C L, STRANGWOOD M. Microstructure-microhardness relationships in friction stir welded AA5251 [J]. Journal of Materials Science, 2007, 42(17): 7299−7306.

[13] GALLAIS C, DENQUIN A, BRÉCHET Y, LAPASSET G. Precipitation microstructures in an AA6056 aluminium alloy after friction stir welding: Characterisation and modelling [J]. Material Science and Engineering A, 2008, 496(1/2): 77−89.

[14] SU J Q, NELSON T W, MISHRA R, MAHONEY M. Microstructural investigation of friction stir welded 7050-T651 aluminium [J]. Acta Materialia, 2003, 51(3): 713−729.

[15] WOO W, BALOGH L, UNGÁR T, CHOO H, FENG Z. Grain structure and dislocation density measurements in a friction-stir welded aluminum alloy using X-ray peak profile analysis [J]. Material Science and Engineering A, 2008, 498(1/2): 308−313.

[16] LIU Hui-jie, FUJII H, MAEDA M, NOGI K. Tensile properties and fracture locations of friction-stir-welded joints of 2017-T351 aluminum alloy [J]. Journal of Materials Processing Technology, 2003, 142(3): 692−696.

[17] CHEN Ying-chun, LIU Hui-jie, FENG Ji-cai. Friction stir welding characteristics of different heat-treated-state 2219 aluminum alloy plates [J]. Material Science and Engineering A, 2006, 420(1/2): 21−25.


**(Edited by FANG Jing-hua)**